Non-uniqueness and symmetry in stratigraphic interpretations: A quantitative approach for determining stratal controls

JIE XIAO[1,2,3] and DAVE WALTHAM[1]

1. Department of Earth Sciences, Royal Holloway University of London, Egham, Surrey TW20 0EX, UK (E-mail: Jie.Xiao.2016@live.rhul.ac.uk)

2. State Key Laboratory of Organic Geochemistry, Guangzhou Institute of Geochemistry, Chinese Academy of Sciences, Guangzhou 510640, China

3. University of Chinese Academy of Sciences, Beijing 100049, China

Associate Editor – Mariano Marzo

Short Title – Non-uniqueness, symmetry and stratigraphy

ABSTRACT

Different combinations of stratal controls could produce identical sequence architectures. Consequently, interpretations of the stratigraphic record, for example to infer palaeo-climate and eustatic sea-level history, suffer from non-uniqueness. However, variations in the multiple controls can be encapsulated through discovery of all possible solutions to an interpretation. As this paper demonstrates, a single solution can be directly transformed into an alternative solution that leaves the expected geological outcomes unaltered, which can be regarded as the existence of symmetry in the interpretation. Repetitive application of the symmetry method can therefore allow additional solutions to be rapidly derived given an existing solution. The proposed method has been adapted to a stratigraphic forward model for interpreting the Baltimore Canyon stratigraphy. Modelling results have indicated the ranges of changes in relative sea-level, sediment supply and subaerial erosion from Oligocene to Mid-Miocene. Using these limits, it is possible to determine what appears to be true in the palaeo-history, even when a solution is not unique.

Keywords: Non-uniqueness, symmetry, sequence stratigraphy, stratal geometries, palaeo-climate.

INTRODUCTION

It has long been understood that siliciclastic depositional systems are controlled on a large scale by subsidence, eustasy and sedimentation (Barrell, 1917; Sloss, 1962). With the increased use of seismic data to image basin margins, these concepts were repackaged as sequence stratigraphy (Vail, 1977; Posamentier et al., 1988) which is an example of inverse observational methods; stratigraphic architectures are observed and stratal controls such as relative sea-level history deduced. However, such an inverse method usually yields non-unique solutions because more than one set of parameters could produce identical observations. The non-uniqueness in the inverse problems can be demonstrated through a metaphor of simple mathematic functions such as $\boldsymbol{x}+\boldsymbol{y}=\boldsymbol{z}$, from which one can never resolve $\boldsymbol{x}$ and $\boldsymbol{y}$ uniquely given only the value of $\boldsymbol{z}$. In the context of sedimentology, assuming $\boldsymbol{x}$ and $\boldsymbol{y}$ are sea-level and sediment supply, respectively, while $\boldsymbol{z}$ is the resulting stratal geometry, it could be hard, if possible, to distinguish the individual influences of the multiple controls.

What makes stratigraphic inverse problems even more challenging is that tectonic and sedimentary processes cannot be simplified as linear functions, and the stratal controls are likely to be strongly correlated rather than independent. Analogue and numerical experiments have shown numerous examples of non-unique stratal geometries. These include transgressive surfaces (e.g. Schlager, 1993; Flemings and Grotzinger, 1996), shoreline trajectories (e.g. Burgess and Prince, 2015), sequence bounding unconformities (e.g. Flemings and Grotzinger, 1996) and aggradational topsets (e.g. Burgess and Allen, 1996; Swenson and Muto, 2007; Prince and Burgess, 2013). Many of these examples were displayed by two-dimensional (2D, i.e. in cross-section) models; however, as strata grow in three-dimensions (3D), the third dimension also needs to be considered on some occasions. Simulating 3D processes can introduce significant extra complications (for example, lobeswitching that leads to asymmetrical delta progradation) and significant additional ways in which the results can be non-unique.

To address the non-uniqueness, sequence stratigraphic studies typically assume accommodation space as the dominant control on any given sedimentary system; moreover, tectonic influences are simplified as monotonic steady subsidence, and sediment supply are considered as a simple function of time (e.g. Posamentier et al., 1988; Van Wagoner et al., 1990; Plint and Nummedal, 2000; Neal and Abreu, 2009). These simplifying assumptions have allowed application of simple models of systems tracts and sequences to reconstruct a relative and perhaps even eustatic sea-level history from selected strata that is then used as a predictive model for stratal patterns in other less well-known areas (Burgess et al., 2006). Numerous problems with this approach have been highlighted (e.g. Heller et al., 1993; Miall, 1997), and the significance of other controls has been recognized. Despite its obvious limitations, this method is still widely applied, either because of its assumed global predictive power or because few practical alternative approaches exist.

However, as evidence for complex tectonic and sediment supply variations mounts (Frostick and Jones, 2002), and as the need increases for robust stratigraphic evidence for palaeo-climate change, a new method is required for determining the multiple controls on stratal patterns that does not depend on simplifying assumptions. Using the principles of symmetry to generate multiple solutions could meet this requirement. This paper shows how the symmetry concept can be adapted to a stratigraphic forward model to produce many possible solutions accounting for the observed sequence architecture. Thus, the use of symmetry methods can provide a more rigorous approach for identifying multiple controls on stratal geometries. To demonstrate the methodology, this paper initially examines 2D models. As a real-case study, the proposed method is applied to interpret the sequence architecture of Oligocene to Mid-Miocene stratigraphy from the Baltimore Canyon trough, New Jersey, USA.

METHOD AND RESULTS

Forward Model

In order to demonstrate and investigate the concept of non-uniqueness in sequence stratigraphy, a computer program, modified from SedTec 2000 (Boylan et al., 2002), has been used to simulate 2Dstratal architectures in response to tectonic and sedimentary effects. Compared with SedTec, an important modification in the new program is that it operates in increments of sediment supply instead of the more conventional approach of stepping forward in constant intervals of time. A source of sediment is assumed to be fixed on the left-hand side of the model. Sediments supplied to the depositional system are classified into coarse-grained and fine-grained. Proportions of the coarse and fine sediment fractions within the initial supply are specified as coarse to fine ratio through time. The abilities of coarse and fine grains to transport are characterized by a variable known as 'transport distance'. Fine grains have a large value of transport distance and travel a long way from the point of supply, whilst coarse grains have a small value of transport distance and settle rapidly. In the forward model, strata either fill up to the sea-surface when there is sufficient sediment to completely fill available accommodation, creating a delta topset, or repose to form a delta foreset. Tectonic rotation effects are also included, of which the hinge point is fixed at the left-edge of the model. The erosion effect in the model is simplified as a subaerial erosion rate, i.e. erosion occurs only above the sea-surface. For more details of the algorithm and its numerical solutions, see Hardy & Waltham (1992), Hardy et al. (1994) and Waltham and Hardy (1995). It is worth noting that forward models applied in this work can be considered as general rather than specific and the methodology presented later for handling non-uniqueness can apply in any type of stratigraphic forward models.

Sea-level versus Sediment Supply

Figure 1 shows an example of strata generated when both sea-level and sediment supply vary through time in a simulated deltaic setting. The identical section can be equally produced by either of the two different solutions (i.e. Fig. 1A and B). Erosion has not been included in this initial, simple case (but will be introduced later). Input sediment was set to be homogeneous in grain-size. Note that sediment supply is cumulative, and thus rate of supply is given by the gradient of the sediment supply curve. This gradient must be non-negative at all times. The remaining part of Fig. 1 shows a 'sea-level versus sediment supply' cross-plot (an SS–SL curve). This can be generated simply by pairing corresponding sea-level and sediment supply values at each point in time. Note that this curve could alternatively be generated directly from observed strata because sea-level through time is indicated by the maximum height at which deposition is occurring whilst cumulative sediment supply is given by the cross-sectional area beneath the corresponding sea floor surface. Crucially, it is also possible to do the reverse and generate the synthetic strata directly from the sea-level and sediment supply pairs. Thus, the cross-section and the SS–SL curves are interchangeable; they are simply two different ways of displaying the same information.

Fundamental to the issue of non-uniqueness is the observation that identical SS–SL curves and therefore, by the argument of interchangeability above, identical stratal architectures, can be generated from different combinations of sediment supply and sea-level curves. This point is illustrated by Fig. 2 which shows how to derive a sea-level curve from an observed architecture given an arbitrary sediment supply. The arbitrary sediment supply curve was constrained only by the need to start at zero, finish at the same final sediment supply as before and to have a non-negative gradient at all times. Once an appropriate sediment supply curve is defined, the corresponding sea-level curve is found by noting that, by definition, the sediment supply curve defines a sediment supply to time conversion. Given this the known SS–SL curve from Fig. 1 can be converted into the required sea-level curve simply by determining which value of sea-level corresponds to the values of sediment supply on the sediment supply curve. Note that there are an infinite number of sediment supply curves that satisfy the start, finish and gradient constraints described above and so there are an infinite number of sediment supply and sea-level combinations corresponding to any given SS–SL curve.

Non-uniqueness and Symmetry

The approach used above to generate multiple solutions to the delta inversion problem can be thought of as exploiting a symmetry in the forward model since it illustrates how different combinations of sea-level and sediment supply can be directly derived whilst the stratal geometry is unaltered. This is similar to rotating a square through 90° and leaving it unchanged. The close relationship between non-uniqueness and a generalized concept of symmetry is widely understood in physics (e.g. Elliott and Dawber, 1979) but is not frequently used in geology. However, a similar analysis has previously been undertaken for a geochemical problem (Waltham and Gröcke, 2006) where it was shown that, although the problem of determining the cause of observed seawater Sr-isotope fluctuations through time has an infinite number of solutions, these are closely related to one another because there is an underlying symmetry.

Symmetry relationships can be used to transform any single solution, once known, into other solutions and therefore gives a practical method for finding large numbers of related solutions. More importantly, the symmetries encapsulate properties of all possible solutions. For example, in the delta-inversion problem discussed above, the symmetry (all solutions have the same SS–SL curve and a monotonic sediment supply curve) implies that all compatible sea-level curves have the same sequence of sea-level highstands and lowstands and only differ in the time-durations between these, i.e. all possible sea-level curves are just horizontally deformed versions of one another, as can be verified by close examination of Fig. 1. Thus, the problem of estimating sea-level history from stratal architecture in the absence of dating information is under-constrained rather than unconstrained, i.e. not all sea-level curves are compatible with the observations even though no single sea-level history can be extracted.

Grain-size Fractions

Application of the symmetry method becomes more difficult if additional controlling factors are included in the model for delta formation. For example, if the factor of multiple grain-sizes is included then the resulting stratal architecture varies according to the relative supplies of each grain size. A coarse-grained delta may have a steeper foreslope than a fine-grained delta and, for a mixed supply, slope may vary with distance. Under these circumstances, the SS–SL curve does not contain sufficient information to allow a complete reconstruction of the architecture. However, the interchangeability argument of the forward model can be extended to include this complication. This can be done by introducing a coarse/fine ratio versus sediment supply cross-plot (SS–CF curve) into the method. Figure 3 shows that identical stratal architectures can be produced by different solutions of sea-level, sediment supply and coarse/fine ratio histories. Both solutions can produce the same SS–SL and SS–CF curves. Similar to the generation of the SS–SL curve, the SS–CF could also be retrieved directly from an observed architecture through careful examination. Thus, the combination of SS–SL and SS–CF curves is interchangeable with the architecture. The combination can then serve as a proxy from which infinite numbers of solutions of sea-level, sediment supply and coarse/fine ratio variations can be derived.

Subaerial Erosion

All of the preceding examples are based on special cases of models in which the strata growth is controlled by variations in accommodation availability but not by the magnitude of sediment supply. A more difficult problem occurs if subaerial erosion is included since, during periods of sea-level fall, material on the delta top may be eroded and subsequently resettled on the delta foreset. As a consequence, maximum heights of sea-level rise are underestimated and much of the sediment reaches its final resting-place with a significant time-delay compared to the time at which it was supplied. Thus, the apparent SS–SL and SS–CF curves produced from examining the architecture no longer agree with the true curves and thus the interchangeability argument breaks down.

However, given an erosive stratigraphic model where the interchangeability does not exist, symmetry of the model can still be exploited using linearization techniques and thus the general principles proposed here remain valid. The procedure can start with a simple solution that assumes no erosion (i.e. erosion rate = 0). A perturbation (i.e. a tiny increment) is then made to the erosion rate, which subsequently causes a residual in the model. The residual caused by the incremental change in erosion rate, however, may be compensated by adjustments in other controls. Successful calculation of the required changes in other parameters can allow the original solution to be modified appropriately and hence the model can be restored. Meanwhile, the original solution is transformed into an alternative solution whilst the model remains unchanged. The new solution can then be used as a basis of the next round of transformation. Repetitive application of the method can allow the original solution to be altered into an infinite number of additional solutions, each of which is associated with a different erosion rate. The workflow of the method is summarized in Fig. 4. The algorithm of the method is given in the Appendix, based on a model controlled by sea-level, sediment supply and subaerial erosion. However, the transformation process is completely general and can be extended to include additional factors (for example, multiple grain-sizes and a more realistic erosion effect as a function of water depth). Note that the transformation method presented here also applies in the simplest deltaic model which involves only sea-level and sediment supply but not erosion. In fact, the non-uniqueness in the simplest model can be demonstrated either by the implicit interchangeability of SS–SL curve and the modelled section or by the transformation process.

Encapsulating Variations in the Controls

An example shown in Fig. 5 demonstrates how a starting solution that assumes no erosion can be transformed into a more realistic solution that assumes a plausible erosion rate. To compensate the erosion effect during subaerial exposure, higher sea-level and additional sediment were required before sea-level fall in order to produce a taller delta profile than the final observation. The additional sediment was then eroded when sea-level dropped below the delta top. Since the delta topset was mainly formed by coarse sediment, the majority of the additional supplies were coarse grains rather than fine grains. When the sediment was eroded from the delta top, it was then reworked and charged into the latter supply, which led to an overestimation of the latter coarse fraction. Consequently, modification is also needed in the coarse/fine ratio curve to leave the architecture unaltered. The three modified curves and the plausible erosion rate hence generate a new solution to the inverse problem. In addition, there could be an infinite number of sediment supply curves, as for the non-erosive case, and each of these give an infinite number of sea-level curves and coarse fraction curves which differ in their history of subaerial exposure episodes.

However, whilst there could be an infinite number of possible solutions to the delta-inverse problem, the problem is not completely unconstrained. As discussed earlier, the gradient of sediment supply curve must be non-negative. When a plausible erosion rate is introduced, increments are required in sediment supply rate during periods of sea-level rise to provide additional sediment. Because the final amount of cumulative sediment supply must remain unchanged, the sediment supply rate during sea-level fall must decrease accordingly. The highest possible erosion rate during delta formation can be found in the solution where the gradient of sediment supply curve is zero at a point of time. Any solution that assumes a higher erosion rate than this value is geologically unfeasible. For the same reason, the sea-level curve in the solution indicates the maximum sea-level heights through time. As a result, upper-bounds can be placed upon the sea-level heights above the erosional surfaces and the associated subaerial erosion rate. Figure 6 shows an instance of how values of upper-bounds and the corresponding solutions are found. It should be noted that these values may vary when alternative (zero-erosion) starting solutions are applied, an example of which is given in Fig. 7.

Using Symmetry for Determining Multiple Controls

The above theoretical treatment, based on a simple numerical forward model of deltaic sequence architecture, demonstrates the application of symmetry concept. It is also possible to determine relative sea-level heights, sediment supply and grain-size fractions from an observed sequence architecture. This would be done using an approach similar to back-stripping (e.g. Sclater and Christie, 1980; Steckler et al., 1993) as follows:

i. Divide the architecture into a number of depositional packages, for example based upon well-defined stratal surfaces.

ii. Successfully strip off each layer by removing any effects due to compaction, rotation, faulting or folding.

iii. As each layer had been successively removed, the apparent (i.e. assuming zero erosion) sediment supply associated with the top depositional package can be estimated by measuring its area (2D) or volume (3D).

iv. The relative sea-level and sediment coarse/fine ratio associated with each package can also be estimated from analysis of stratal terminations like onlap and toplap, as well as from a shoreline trajectory analysis (Helland-Hansen and Hampson, 2009).

v. The successive sediment supply (from iii) and sea-level (from iv) pairs can be applied to produce an apparent SS–SL curve. Similarly, an SS–CF curve can also be generated using the sediment supply and coarse/fine ratio (from iv) pairs.

vi. The SS–SL and SS–CF curves can then be combined with an arbitrarily chosen sediment supply curve to give the corresponding sea-level curve and coarse/fine ratio curve. This step can be repeated for any number of appropriate sediment supply guesses.

vii. The initial (i.e. zero-erosion) models are then modified for finite erosion using the approach shown in Fig. 4.

A diagram illustrating the back-stripping procedure [i.e. steps (i) to (iv) in the approach] can be found in (Steckler et al., 1993). A significant advantage of this method is that it allows generation of relative sea-level, sediment supply and coarse/fine ratio values that can account for the observed strata. If dating estimates are available for the depositional packages, then it becomes possible to constrain the sediment supply curve used in step (vi). Consequently, the relative sea-level and coarse/fine ratio curves also become constrained. Note that the resulting histories are not based upon an unrealistic assumption of constant sediment supply.

Some of these steps in defining values of relative sea-level, sediment supply and coarse/fine ratio may not be straightforward. First, measurement of sediment amount in each stratal package relies on successful restoration of the strata and accurate identification of the depositional packages. Secondly, estimation of sea-level elevation through time requires careful identification of appropriate stratal terminations, and careful consideration of evidence for abnormal subaerial exposure of marine strata that occurs during forced regression, which is the only reliable indicator of relative sea-level fall. In the absence of abnormal subaerial exposure many stratal patterns can be equally well explained by sediment supply variations driving transgression and 'unforced' regression (Schlager, 1993). In addition, the process of determining coarse/fine ratio that accounts for each stratal package is iterative, which would be done by: (1) defining an initial guess for the coarse-grained proportion and running the forward model, (2) comparing the output with the observation and calculating the errors, (3) adjusting the initial values to reduce the errors, and then (4) running the model again and repeating this procedure until an acceptable match is achieved between the resulting model and observed architecture. Any inaccurate estimation of the controlling factors that account for the depositional packages can lead to the production of an incorrect starting solution and hence an incorrect range of variations in stratal controls.

Baltimore Canyon: A Real-world Example

The techniques discussed above have been applied to interpret the Oligocene to Mid-Miocene stratigraphy from Baltimore Canyon Trough, offshore New Jersey. The Baltimore Canyon stratigraphy can be effectively viewed as a 2D system. A cross-section of the stratigraphy has been observed from a seismic reflection profile *Ewing* 9009, line 1003. The strata section is arranged into a series of 15 depositional packages according to the stratal line interpretation from Steckler et al. (1999), whereas the duration of the whole section is estimated to be 33.0 Ma to 11.5 Ma according to δ^{18}O record analysis from Miller et al. (1998). The seismic reflection profile of the stratigraphy, identification of depositional packages and the dating estimates are shown in Fig. 8.

The case study began with an arbitrary solution that assumes no erosion had occurred during the Baltimore Canyon stratigraphy development. The back-stripping approach was applied to remove the tectonic effects on the strata and to determine changes in relative sea-level, sediment supply and coarse/fine ratio through time. Dating estimates correlated with the depositional packages were then applied and therefore the curves of these controlling factors were produced (Fig. 9A). Note that variations in the stratal controls during ages between each pair of the adjacent surfaces are still unknown. To estimate the uncertainties in the starting solution, conservative error bars have been attached with one of the points in the sediment supply curves. The three curves, incorporated with strata rotation angle though time determined from the back-stripping process, were then used to generate a synthetic architecture from the forward model (Fig. 9B). Comparison of Fig. 8 and Fig. 9B indicates that a good match has been achieved between the observed stratal geometry and the modelled section.

Next, subaerial erosion was introduced into the model and symmetry transformations were applied to adjust the input parameters for restoration of the resulting architecture. The increment of subaerial erosion rate in each step was set at 0.1 m/Myr. Figure 9C shows that when the erosion rate reached 30 m/Myr, the sediment supply rate at 15 Ma was found to be zero. This indicates the upper-bounds upon the subaerial erosion rate and upon the highest possible relative sea-level that could have existed during the strata growth. Compared with the original solution, differences in relative sea-level height can be up to 50 m during relative sea-level rising stage. This suggests that even a small change in the assumed subaerial erosion rate can leave a notable impact on the inferred palaeo-history. Note that, as discussed earlier, in the absence of dating estimated for the strata, the starting solution is also non-unique and can result in rather different solutions for the inference.

DISCUSSION

Historically, geologists have realized that stratal geometries formed in siliciclastic shallow-marine environments are determined by the interaction of multiple controls, not just the accommodation. With the aid of quantitative forward models, stratal controls can be parameterized and then be used for stratigraphic simulations. Numerous attempts have been made to generate a solution that can produce a 'best-fit' model of the observed stratal geometry (e.g. Bornholdt et al., 1999; Cross and Lessenger, 1999; Wijns et al., 2004; Charvin et al., 2009). However, any single solution found by these approaches can be considered a local optima (Burgess et al., 2012) and there are likely to be many others. Despite the awareness, entire exploration of the parameter space has not proved to be available, either using exhaustive searching approaches or by defining different starting guesses for the inversion algorithm.

This paper illustrates how to exploit the symmetry from a stratigraphic model and thus to transform an existing solution into the additional ones that can produce the same model outputs. However, as (Burton et al., 1987) claimed, it is impossible to determine the real solution from all possible solutions due to the absence of geological reason for distinguishing the effects of individual controls. Although all of these solutions appear to be possible, they may imply very different tectono-sedimentary processes and very different palaeo-history. Therefore, application of simple assumptions, such as constant sediment supply rate through time, is untenable. To rely on any single interpretation of a stratigraphy can lead to substantial uncertainties in the palaeo-history reconstruction. In an inverse problem, the conventional forward modelling approach that a model conducts in constant time interval should also be avoided, since it implies an assumption that the time-steps between each of the stratal surfaces are identical. In comparison, a model that operates in cumulative sediment supply, same as the one employed in this work, is more appropriate in this context.

Nevertheless, discovery of useful information from stratigraphic inversion is possible. Transformation based on the principles of symmetry shows that all the solutions are closely related. In this work, for example, all sea-level curves produced from the same strata architecture have the same sequence of sea-level highstand/lowstand system tracts and only differ in their amplitude and durations. If dating estimates are available for the strata, the timing of highstands and lowstands also become constrained. Given the only requirement that sediment supply rate must be non-negative, quantitative limits can be placed on the relative sea-level amplitude and on the subaerial erosion rate. Properties calculated from the method that are common to all solutions must be true of the real solution whatever it is. This is similar to the conclusions of Heller et al. (1993) and Waltham and Gröcke (2006). However, although these investigated the joint effects of multiple controls and estimated the range of variations in the individual factors, both studies assumed that one of the multiple controls is dominant whilst the others either remain constant or change independently. Such an assumption is unlikely to be realistic in real-world geology since the various controls are often significantly correlated. Using symmetry transformation can overcome this problem well since multiple parameters can be altered simultaneously and thus the competing effects of the stratal controls can be unravelled.

A real-case study has been conducted based on the subsurface data of Oligocene to Mid-Miocene deposits in Baltimore Canyon. Sequence architecture of the stratigraphy have been previously examined and several scenarios of eustasy, sediment supply history and tectonic history have been reconstructed (e.g. Posamentier et al., 1988; Van Wagoner et al., 1990; Miller et al., 1998). These interpretations have been verified using numerical models which prove that close matches were generated between the resulting model and the observation of strata (e.g. Lawrence et al., 1990; Schroeder and Greenlee, 1993; Poulsen et al., 1998; Steckler et al., 1999). However, model work presented here shows that an infinite number of alternative scenarios could be used to reproduce the same sequence architecture. Some differences can be observed between the inference herein and the scenarios of reconstruction in the previous studies, and the maximum relative sea-level and maximum erosion rate suggested here may not be necessary to explain the formation of the stratigraphic architecture. However, these make no contradiction to the issue that identical observations could be produced by different histories. Hence the whole range of solutions, rather than a single solution, should be considered in an interpretation. Nevertheless, several statements must be true according to this model work. Whatever the real solution is:

1. The Baltimore Canyon stratigraphy has been shown to undergo a slight erosion subaerial erosion (erosion rate≤30 m/Myr) throughout the modelled period.
2. Two sharp changes (rapid fall followed by rapid rise) have been found in relative sea-level history, respectively at 16 Ma and 13 Ma.
3. Large proportions of coarse siliciclastic (coarse/fine ratio ≥8) have been shown to occur in 15 Ma and 12 Ma.

This paper also shows that increasing sophistication of a stratigraphic model could make the model less unique. In the simplest model (i.e. the one controlled only by sea-level change and sediment supply), given any appropriate sediment supply curve, there is a corresponding sea-level curve. If dating estimates for the stratal surfaces are available, then a particular sediment supply curve is defined and hence the corresponding sea-level curve can be found. However, once the subaerial erosion effect is introduced into the model, for each of the given subaerial erosion rates, there are an infinite number of apparent sediment supply curves, each of these has a corresponding sea-level curve. Therefore, the model becomes even less unique. Since the simulation of depositional system is significantly simplified compared with real-world geology, it is reasonable to suspect that stratigraphic interpretations could suffer from even more serious non-uniqueness when additional factors are included. As a useful tool, the principles of symmetry are general and simple enough to be widely applicable in higher dimensional and more sophisticated models. The symmetry method therefore bears great potential in the inference of palaeo-history from stratal geometries formed in various tectono-sedimentary settings observed from outcrop or subsurface.

CONCLUSIONS

Non-uniqueness is a key challenge in sequence stratigraphy. In this paper, a forward model of delta formation illustrates that the same stratal geometry can be generated using different combinations of parameters. The non-unique results suggest that the simplifying assumptions used in most current applications of the sequence stratigraphic method is untenable. However, the symmetry method proposed in this work here has been shown to be a useful tool for determining multiple controls on stratal geometries. In a stratigraphic model, symmetries provide rules for transforming model parameters in ways which leave the resulting geometry unaltered. Using this insight, it is possible to derive all possible solutions from an existing solution. Calculation of multiple solutions can allow properties common to all solutions, and hence to the unknown correct one, to be found. Consequently, application of the symmetry method offers more complete solutions to the interpretation of stratal geometries and hence more predictive power. Application of the method also allows more robust interpretation of the controls on strata geometries and hence generation of more reliable data, for example for palaeo-climate studies.

ACKNOWLEDGEMENT

Associate Editor Mariano Marzo and two reviewers, Gary Nichols and Kerry Gallagher, are thanked for their valuable comments that greatly helped to strengthen the manuscript. The authors would like to thank Saswata Hier-Majumder and YunPeng Wang for their useful discussions during the manuscript preparation. Jie Xiao acknowledges the support provided by China Scholarship Council (CSC).

REFERENCES

Barrell, J. (1917) Rhythms and the measurements of geologic time. *Bulletin of the Geological Society of America*, **28,** 745-904.

Bornholdt, S., Nordlund, U. and Westphal, H. (1999) Inverse stratigraphic modeling using genetic algorithms.

Boylan, A., Waltham, D., Bosence, D., Badenas, B. and Aurell, M. (2002) Digital rocks: linking forward modelling to carbonate facies. *Basin Research*, **14,** 401-415.

Burgess, P. and Allen, P. (1996) A forward-modelling analysis of the controls on sequence stratigraphical geometries. *Geological Society, London, Special Publications*, **103,** 9-24.

Burgess, P.M., Lammers, H., van Oosterhout, C. and Granjeon, D. (2006) Multivariate sequence stratigraphy: Tackling complexity and uncertainty with stratigraphic forward modeling, multiple scenarios, and conditional frequency maps. *AAPG bulletin*, **90,** 1883-1901.

Burgess, P.M. and Prince, G.D. (2015) Non‐unique stratal geometries: implications for sequence stratigraphic interpretations. *Basin Research*, **27,** 351-365.

Burton, R., Kendall, C.G.S.C. and Lerche, I. (1987) Out of our depth: on the impossibility of fathoming eustasy from the stratigraphic record. *Earth-Science Reviews*, **24,** 237-277.

Charvin, K., Gallagher, K., Hampson, G.L. and Labourdette, R. (2009) A Bayesian approach to inverse modelling of stratigraphy, part 1: Method. *Basin Research*, **21,** 5-25.

Cross, T.A. and Lessenger, M.A. (1999) Construction and application of a stratigraphic inverse model.

Elliott, J. and Dawber, P. (1979) *Symmetry in Physics, Volume 1 and 2*. Macmillan Press, London, 280 pp.

Flemings, P.B. and Grotzinger, J.P. (1996) STRATA: Freeware for analyzing classic stratigraphic problems. *GSA Today*, **6,** 1-7.

Frostick, L.E. and Jones, S.J. (2002) Impact of periodicity on sediment flux in alluvial systems: grain to basin scale. *Geological Society, London, Special Publications*, **191,** 81-95.

Hardy, S., Dart, C.J. and Waltham, D. (1994) Computer modelling of the influence of tectonics on sequence architecture of coarse-grained fan deltas. *Marine and Petroleum Geology*, **11,** 561-574.

Hardy, S. and Waltham, D. (1992) Computer modeling of tectonics, eustacy, and sedimentation using the Macintosh. *Geobyte*, **7,** 42-42.

Helland-Hansen, W. and Hampson, G. (2009) Trajectory analysis: concepts and applications. *Basin Research*, **21,** 454-483.

Heller, P.L., Burns, B.A. and Marzo, M. (1993) Stratigraphic solution sets for determining the roles of sediment supply, subsidence, and sea level on transgressions and regressions. *Geology*, **21,** 747-750.

Lawrence, D.T., Doyle, M. and Aigner, T. (1990) Stratigraphic Simulation of Sedimentary Basins: Concepts and Calibration (1). *Aapg Bulletin*, **74,** 273-295.

Miall, A.D. (1997) *The geology of stratigraphic sequences*. Springer-Verlag, Berlin, 433 pp.

Miller, K.G., Mountain, G.S., Browning, J.V., Kominz, M., Sugarman, P.J., Christie‐Blick, N., Katz, M.E. and Wright, J.D. (1998) Cenozoic global sea level, sequences, and the New Jersey transect: results from coastal plain and continental slope drilling. *Reviews of Geophysics*, **36,** 569-601.

Neal, J. and Abreu, V. (2009) Sequence stratigraphy hierarchy and the accommodation succession method. *Geology*, **37,** 779-782.

Plint, A.G. and Nummedal, D. (2000) The falling stage systems tract: recognition and importance in sequence stratigraphic analysis. *Geological Society, London, Special Publications*, **172,** 1-17.

Posamentier, H., Jervey, M. and Vail, P. (1988) Eustatic controls on clastic deposition I—conceptual framework.

Poulsen, C.J., Flemings, P.B., Robinson, R.A. and Metzger, J.M. (1998) Three-dimensional stratigraphic evolution of the Miocene Baltimore Canyon region: Implications for eustatic interpretations and the systems tract model. *Geological Society of America Bulletin*, **110,** 1105-1122.

Prince, G.D. and Burgess, P.M. (2013) Numerical modeling of falling-stage topset aggradation: implications for distinguishing between forced and unforced regressions in the geological record. *Journal of Sedimentary Research*, **83,** 767-781.

Schlager, W. (1993) Accommodation and supply—a dual control on stratigraphic sequences. *Sedimentary Geology*, **86,** 111-136.

Schroeder, F.W. and Greenlee, S.M. (1993) Testing eustatic curves based on Baltimore Canyon Neogene stratigraphy: An example application of basin-fill simulation. *AAPG Bulletin*, **77,** 638-656.

Sclater, J.G. and Christie, P.A. (1980) Continental stretching: An explanation of the post‐Mid‐Cretaceous subsidence of the central North Sea Basin. *Journal of Geophysical Research: Solid Earth*, **85,** 3711-3739.

Sloss, L. (1962) Stratigraphic models in exploration. *Journal of Sedimentary Research*, **32**.

Steckler, M., Reynolds, D., Coakley, B., Swift, B. and Jarrard, R. (1993) Modelling passive margin sequence stratigraphy. *Sequence stratigraphy and facies associations***,** 19-41.

Steckler, M.S., Mountain, G.S., Miller, K.G. and Christie-Blick, N. (1999) Reconstruction of Tertiary progradation and clinoform development on the New Jersey passive margin by 2-D backstripping. *Marine Geology*, **154,** 399-420.

Swenson, J.B. and Muto, T. (2007) Response of coastal plain rivers to falling relative sea ‐ level: allogenic controls on the aggradational phase. *Sedimentology*, **54,** 207-221.

Vail, P.R. (1977) Seismic stratigraphy and global changes of sea level. *Bull. Am. Assoc. Petrol. Geol., Mem.*, **26,** 49-212.

Van Wagoner, J.C., Mitchum, R., Campion, K. and Rahmanian, V. (1990) Siliciclastic sequence stratigraphy in well logs, cores, and outcrops: concepts for high-resolution correlation of time and facies.

Waltham, D. and Gröcke, D.R. (2006) Non-uniqueness and interpretation of the seawater 87Sr/86Sr curve. *Geochimica et Cosmochimica Acta*, **70,** 384-394.

Waltham, D. and Hardy, S. (1995) The velocity description of deformation. Paper 1: theory. *Marine and petroleum geology*, **12,** 153-163.

Wijns, C., Poulet, T., Boschetti, F., Dyt, C. and Griffiths, C. (2004) Interactive inverse methodology applied to stratigraphic forward modelling. *Geological Society, London, Special Publications*, **239,** 147-156.

APPENDIX

A stratigraphic forward model controlled by sediment supply, sea-level and subaerial erosion can be formulated as $\boldsymbol{H} = f(\boldsymbol{SS}, \boldsymbol{SL}, e)$, where $\boldsymbol{H} = (h_{11}, h_{12}, \dots, h_{1N}, h_{21}, h_{22}, \dots, h_{2N}, h_{M1}, h_{M2}, \dots, h_{MN})^T$ is an observed stratal geometry described by the heights of the M stratal surfaces at N horizontal positions; $\boldsymbol{SS} = (ss_1, ss_2, \dots, ss_M)^T$ and $\boldsymbol{SL} = (sl_1, sl_2, \dots, sl_M)^T$ are respectively sediment supply and sea-level accounting for the stratal surfaces; e is the subaerial erosion rate.

When a perturbation (Δe) is given to the subaerial erosion rate, a residual is subsequently caused in the model. The residual, however, may be compensated by appropriate adjustments in sediment supply ($\Delta \boldsymbol{SS}$) and sea-level ($\Delta \boldsymbol{SL}$). Using first-order Taylor Series, this can be expressed as:

$$\boldsymbol{d} + \nabla_{\boldsymbol{SS}} f(\boldsymbol{SS}, \boldsymbol{SL}, e) \cdot \Delta \boldsymbol{SS} + \nabla_{\boldsymbol{SL}} f(\boldsymbol{SS}, \boldsymbol{SL}, e) \cdot \Delta \boldsymbol{SL} = \boldsymbol{\rho} \tag{1}$$

, where $\boldsymbol{d} = f(\boldsymbol{SS}, \boldsymbol{SL}, e + \Delta e) - f(\boldsymbol{SS}, \boldsymbol{SL}, e)$ is the residual caused by Δe; $\nabla_{\boldsymbol{SS}} f(\boldsymbol{SS}, \boldsymbol{SL}, e)$, $\nabla_{\boldsymbol{SL}} f(\boldsymbol{SS}, \boldsymbol{SL}, e)$ are partial derivatives with respect to $\boldsymbol{SS}$ and $\boldsymbol{SL}$ and can be calculated from the forward model using finite difference method; $\boldsymbol{\rho}$ is the term of remainder. If $\boldsymbol{d}$ could be well compensated by $\Delta \boldsymbol{SS}$ and $\Delta \boldsymbol{SL}$ then $\boldsymbol{\rho} \to \boldsymbol{0}$. Note that $\boldsymbol{d}$ is a matrix in size of $M \times N$, whilst $\Delta \boldsymbol{SS}$ and $\Delta \boldsymbol{SL}$ are both vectors with a length of M. Every element in $\Delta \boldsymbol{SS}$ and $\Delta \boldsymbol{SL}$ can make a difference in the model and hence $\nabla_{\boldsymbol{SS}} f(\boldsymbol{SS}, \boldsymbol{SL}, e)$ and $\nabla_{\boldsymbol{SL}} f(\boldsymbol{SS}, \boldsymbol{SL}, e)$ are both matrices in size of $M \times N \times M$.

Let $\mathrm{A} = \nabla_{\boldsymbol{SS}} f(\boldsymbol{SS}, \boldsymbol{SL}, e)$ and $\mathrm{B} = \nabla_{\boldsymbol{SL}} f(\boldsymbol{SS}, \boldsymbol{SL}, e)$. Writing the equation in full gives:

$$\sum_{i=1}^{M\times N} \left(d_i + \sum_{j=1}^{M} A_{ij}\, \Delta ss_j + \sum_{j=1}^{M} B_{ij}\, \Delta sl_j \right) = \sum_{i=1}^{M\times N} \rho_i \tag{2}$$

Thus, there are $M \times N$ equations and $M \times 2$ unknowns (i.e. the M elements in $\Delta \boldsymbol{SS}$ and the M elements in $\Delta \boldsymbol{SL}$). Provided $N \gg 2$, the problem of solving $\Delta \boldsymbol{SS}$ and $\Delta \boldsymbol{SL}$ from Eq. 2 is over-determined. Using least square solution, the square error of Eq. 2 can be calculated as:

$$\boldsymbol{\rho}^2 = \sum_{i=1}^{M\times N} \rho_i^2 = \sum_{i=1}^{M\times N} \left(d_i + \sum_{j=1}^{M} A_{ij} \Delta ss_j + \sum_{j=1}^{M} B_{ij} \Delta sl_j \right)^2 \tag{3}$$

To minimize $\boldsymbol{\rho}$, set $\partial \boldsymbol{\rho}^2 / \partial \Delta ss_k = 0$ and $\partial \boldsymbol{\rho}^2 / \partial \Delta sl_l = 0$ $(k, l = 1, 2, \dots, M)$:

$$\begin{cases} 2 \cdot \sum_{i=1}^{M\times N} \left(d_i + \sum_{j=1}^{M} A_{ij} \Delta ss_j + \sum_{j=1}^{M} B_{ij} \Delta sl_j \right) \cdot A_{ik} = 0 \\ 2 \cdot \sum_{i=1}^{M\times N} \left(d_i + \sum_{j=1}^{M} A_{ij} \Delta ss_j + \sum_{j=1}^{M} B_{ij} \Delta sl_j \right) \cdot B_{il} = 0 \end{cases} \tag{4}$$

, which may be rearranged as:

$$\begin{cases} \sum_{i=1}^{M\times N} A_{ik} d_i + \sum_{j=1}^{M} \sum_{i=1}^{M\times N} A_{ik} A_{ij} \Delta ss_j + \sum_{j=1}^{M} \sum_{i=1}^{M\times N} A_{ik} B_{ij} \Delta sl_j = 0 \\ \sum_{i=1}^{M\times N} B_{il} d_i + \sum_{j=1}^{M} \sum_{i=1}^{M\times N} B_{il} A_{ij} \Delta ss_j + \sum_{j=1}^{M} \sum_{i=1}^{M\times N} B_{il} B_{ij} \Delta sl_j = 0 \end{cases} \tag{5}$$

Equation 5 may be written in matrix notation:

$$\begin{cases} \mathrm{A^T} \boldsymbol{d} + \mathrm{A^T A} \cdot \Delta \boldsymbol{SS} + \mathrm{A^T B} \cdot \Delta \boldsymbol{SL} = \boldsymbol{0} \\ \mathrm{B^T} \boldsymbol{d} + \mathrm{B^T A} \cdot \Delta \boldsymbol{SS} + \mathrm{B^T B} \cdot \Delta \boldsymbol{SL} = \boldsymbol{0} \end{cases} \tag{6}$$

Therefore, the least square solution to eq. (1) is:

$$\begin{cases} \Delta \boldsymbol{SS} = [(\mathrm{B^T B})^{-1} \mathrm{B^T A} - (\mathrm{A^T B})^{-1} \mathrm{A^T A}]^{-1} \cdot [(\mathrm{A^T B})^{-1} \mathrm{A^T} - (\mathrm{B^T B})^{-1} \mathrm{B^T}] \cdot \boldsymbol{d} \\ \Delta \boldsymbol{SL} = [(\mathrm{A^T A})^{-1} \mathrm{A^T B} - (\mathrm{B^T A})^{-1} \mathrm{B^T B}]^{-1} \cdot [(\mathrm{B^T A})^{-1} \mathrm{B^T} - (\mathrm{A^T A})^{-1} \mathrm{A^T}] \cdot \boldsymbol{d} \end{cases} \tag{7}$$

Given the above $\Delta \boldsymbol{SS}$ and $\Delta \boldsymbol{SL}$, $f(\boldsymbol{SS} + \Delta \boldsymbol{SS}, \boldsymbol{SL} + \Delta \boldsymbol{SL}, e + \Delta e) = f(\boldsymbol{SS}, \boldsymbol{SL}, e)$ and hence the model remains unaltered.

FIGURES

Fig. 1. Two sets of sediment supply and sea-level curves (A) and (B) are plotted with the resulting strata geometry from a simple 2D forward model of delta formation, and a cross-plot of sediment supply versus sea-level (SS–SL curve). Note that ka = thousands of years ago (an age). Different histories of sea-level and sediment supply can generate exactly the same stratal geometry, demonstrating non-uniqueness.

Fig. 2. A flow chart illustrating how principles of symmetry can be used to derive multiple interchangeable sediment supply and sea-level curves from a stratal geometry. Observation on stratal geometry (A) is used to derive a SS–SL curve (B). Two sediment supply curves (C) and (D) are derived from the observed geometry constrained by required sediment supply magnitude and by conservation of mass, and the symmetry encoded in the SS–SL curve is used to derive a sea-level curve for each of these sediment supply curves (E) and (F). The resulting pair of sediment supply curve and sea-level curve can generate identical stratal geometry as seen in (A).

Fig. 3. Non-uniqueness and symmetry in a more sophisticated model including multiple grain-sizes. The two solutions of relative sea-level curve, sediment supply curves and coarse/fine ratio curves can produce identical stratal geometry, SS–SL curve and cross-plot of sediment supply versus coarse/fine ratio (SS–CF curve). All additional solutions can be generated using the combination of SS–SL and SS–CF curves.

Fig. 4. A flow chart demonstrating how to generate all possible solutions for a non-unique stratigraphic inverse problem. *The maximum erosion rate is defined by the assumed erosion rate in the solution where the gradient of cumulative sediment supply curve is 0 at a time. As the sediment supply rate must always be non-negative, no further increment could be made to the assumed erosion rate. Hence, the erosion rate in this solution is the highest possible subaerial erosion rate.

Fig. 5. Using the symmetry method, a starting solution that assumes no erosion (black dotted curves) can be modified into an alternative solution with a plausible erosion rate (red solid curves). Note that kyr = thousands of years (a duration). Stratal geometries produced by the two solutions are identical.

Fig. 6. Another alternative solution (red solid curves) modified from the starting solution (black dotted curves). The gradient of the sediment supply curve in *ca* 35 ka of modelled period is shown to be 0, which suggests a sediment supply rate of 0 at this point of time. The erosion rate presented here is the highest possible erosion rate whilst the corresponding sea-level curve indicates the highest possible sea-level amplitude through time.

Fig. 7. Using different starting solution can result in different sets of additional solutions. Note that upper-bounds upon sea-level height and upon associated erosion rate in each of the solution sets may also vary.

Fig. 8. Sequence architecture of Baltimore Canyon Oligocene to Mid-Miocene stratigraphy observed from depth-converted seismic section *Ewing* 9009, line 1003 [modified from Steckler et al. (1999)].

Fig. 9. (A) A starting solution of sediment supply, relative sea-level and coarse/fine ratio from the Oligocene to Mid-Miocene reconstructed from Baltimore Canyon stratigraphy assuming no erosion. The inferred palaeo-history is constrained by dating estimates (makers shown on the sediment supply curve) for the strata. An error bar on both timing and height are used to estimate maximum of variability in sediment supply history one could infer from the observed data. (B) A synthetic architecture generated from a forward model using the starting solution. (C) An alternative solution that accounts for identical architecture is modified from the starting solution using the symmetry method. This solution indicates the upper-bounds upon relative sea-level height through time and upon the associated erosion rate. Note that Ma = millions of years ago (an age) and Myr = millions of years (a duration).

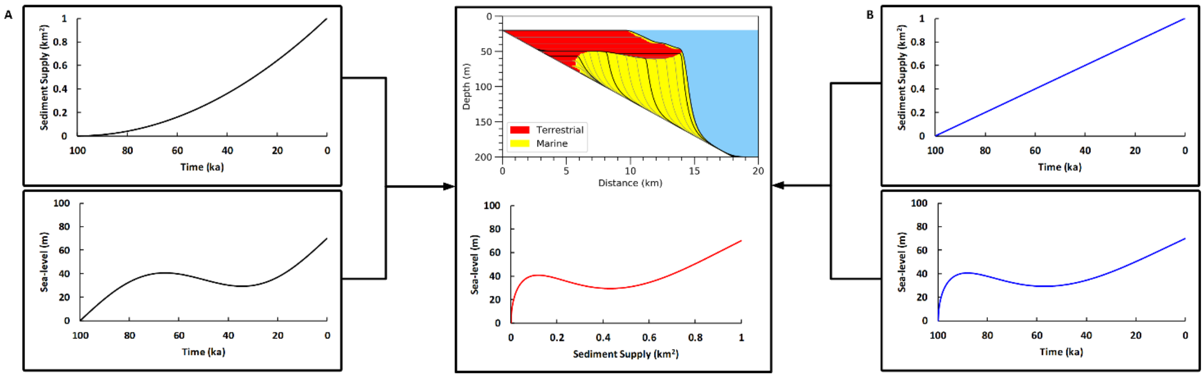

A
Sediment Supply (km²)
Time (ka)
Sea-level (m)
Depth (m)
Distance (km)
Terrestrial
Marine
Sediment Supply (km²)
B

Figure 1

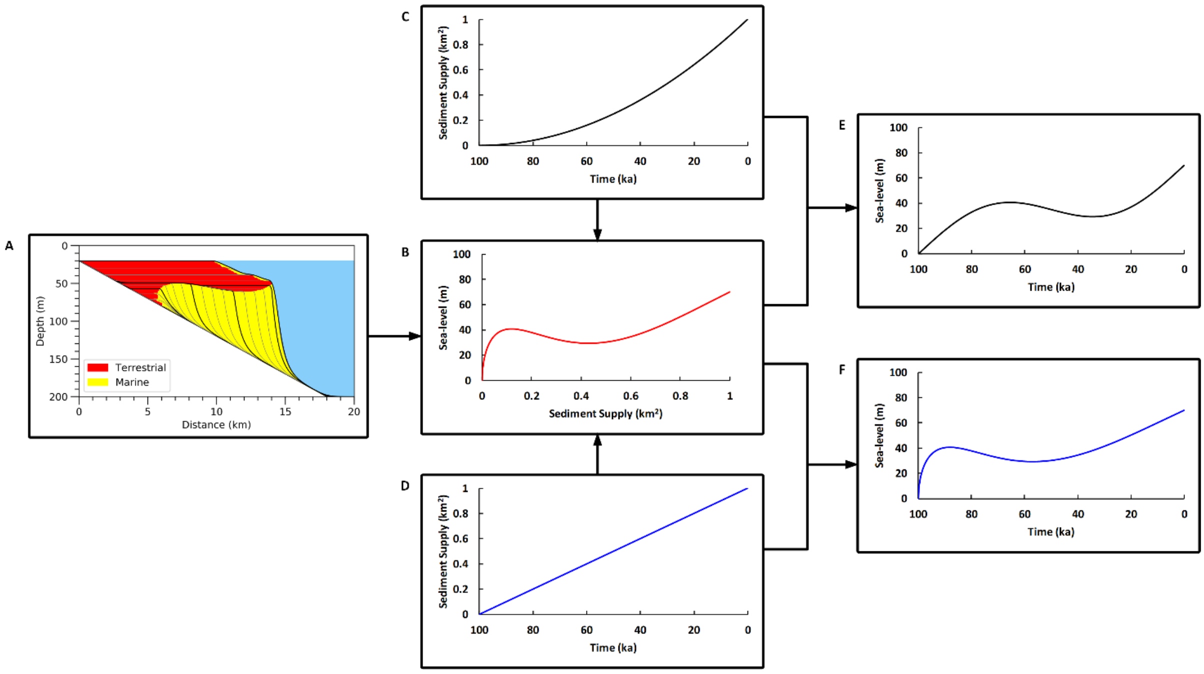
C
Sediment Supply (km²)
Time (ka)
B
Sea-level (m)
Sediment Supply (km²)
D
Sediment Supply (km²)
Time (ka)
A
Depth (m)
Distance (km)
Terrestrial
Marine
E
Sea-level (m)
Time (ka)
F
Sea-level (m)
Time (ka)

Figure 2

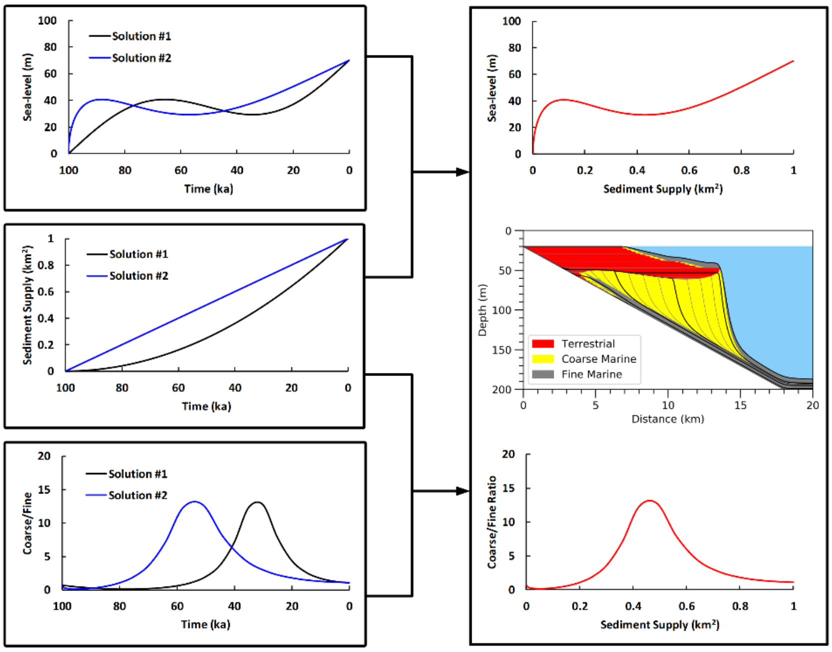

Solution #1
Solution #2
Sea-level (m)
Time (ka)
Sediment Supply (km²)
Coarse/Fine
Sediment Supply (km²)
Depth (m)
Distance (km)
Terrestrial
Coarse Marine
Fine Marine
Coarse/Fine Ratio

Figure 3

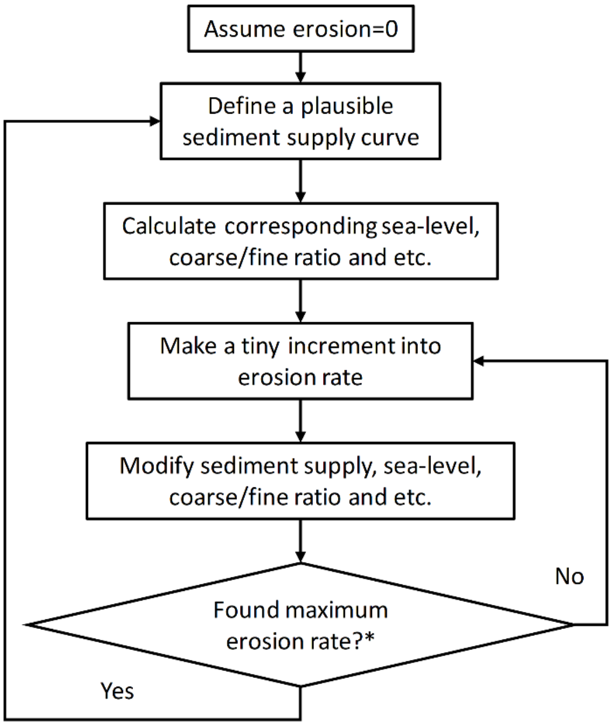
Assume erosion=0
Define a plausible sediment supply curve
Calculate corresponding sea-level, coarse/fine ratio and etc.
Make a tiny increment into erosion rate
Modify sediment supply, sea-level, coarse/fine ratio and etc.
Found maximum erosion rate?*
No
Yes

Figure 4

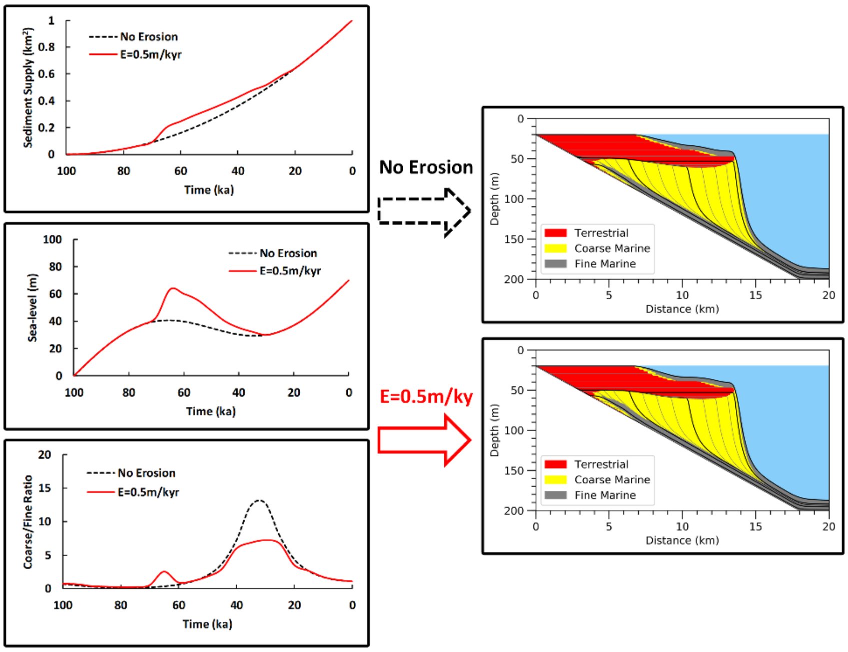
No Erosion
E=0.5m/kyr
Sediment Supply (km²)
Time (ka)
Sea-level (m)
Coarse/Fine Ratio
No Erosion
E=0.5m/ky
Depth (m)
Distance (km)
Terrestrial
Coarse Marine
Fine Marine

Figure 5

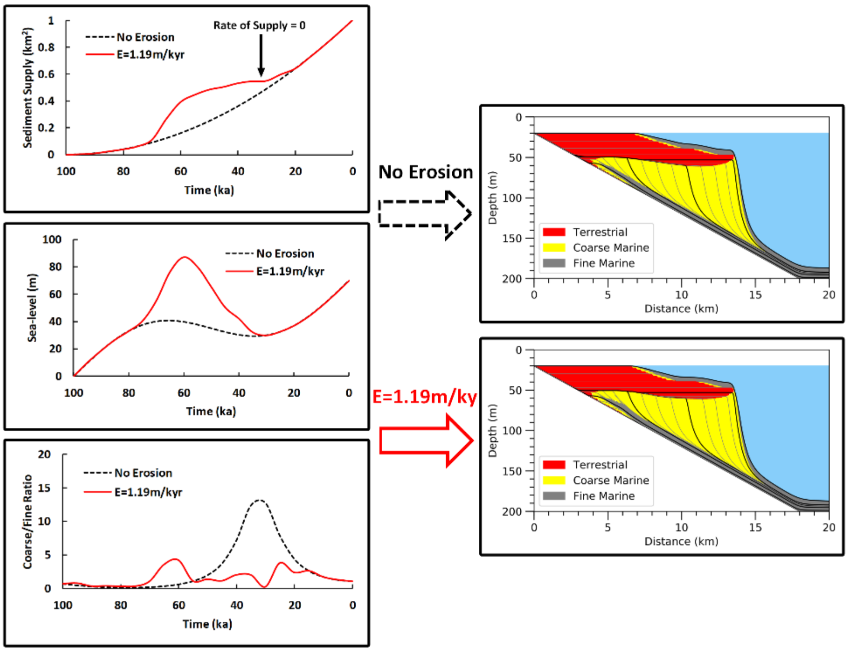

Sediment Supply (km²)
Rate of Supply = 0
No Erosion
E=1.19m/kyr
Time (ka)
Sea-level (m)
Coarse/Fine Ratio
No Erosion
E=1.19m/ky
Depth (m)
Distance (km)
Terrestrial
Coarse Marine
Fine Marine

Figure 6

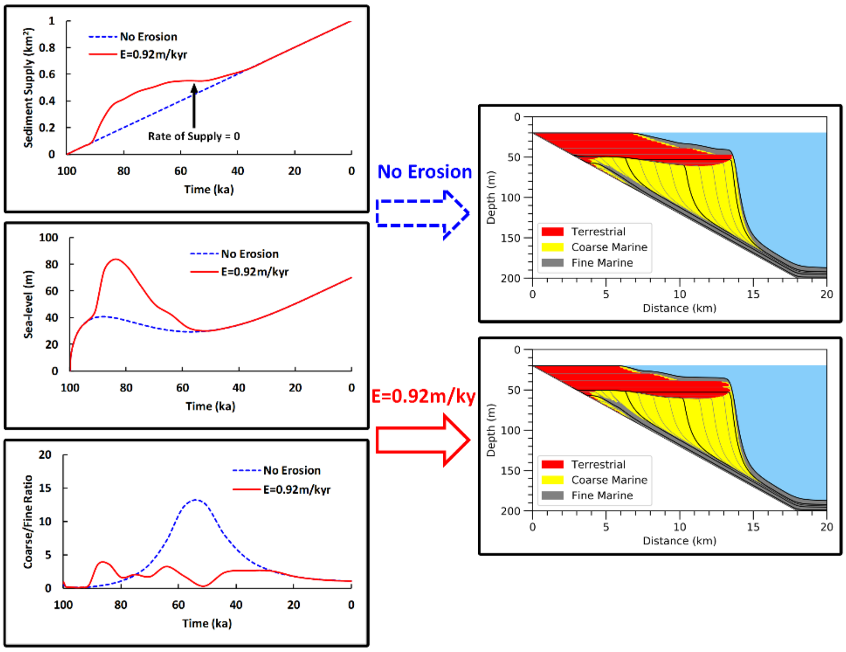

No Erosion
E=0.92m/kyr
Sediment Supply (km²)
Rate of Supply = 0
Time (ka)
Sea-level (m)
Coarse/Fine Ratio
No Erosion
E=0.92m/ky
Depth (m)
Distance (km)
Terrestrial
Coarse Marine
Fine Marine

Figure 7

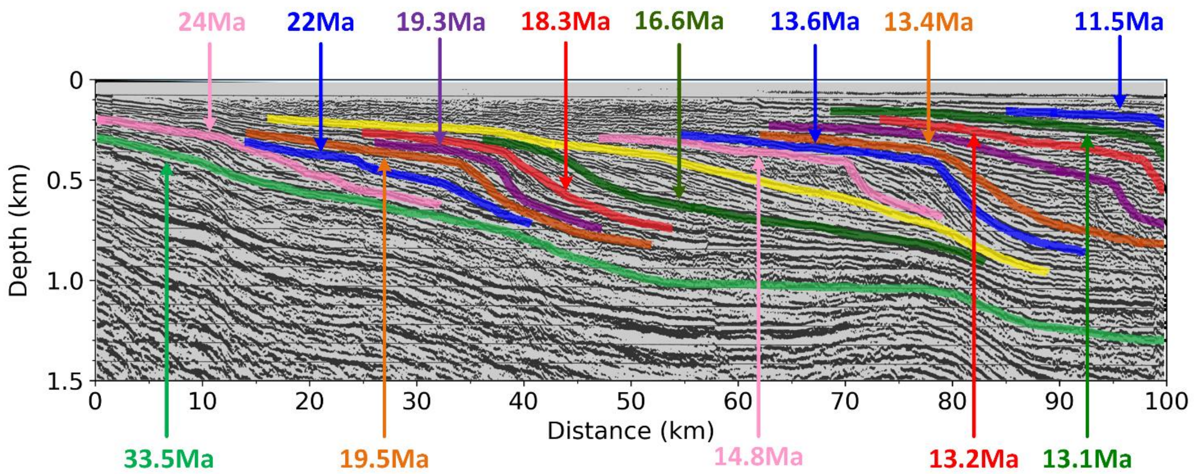
24Ma
22Ma
19.3Ma
18.3Ma
16.6Ma
13.6Ma
13.4Ma
11.5Ma
Depth (km)
0
0.5
1.0
1.5
0
10
20
30
40
50
60
70
80
90
100
Distance (km)
33.5Ma
19.5Ma
14.8Ma
13.2Ma
13.1Ma

Figure 8

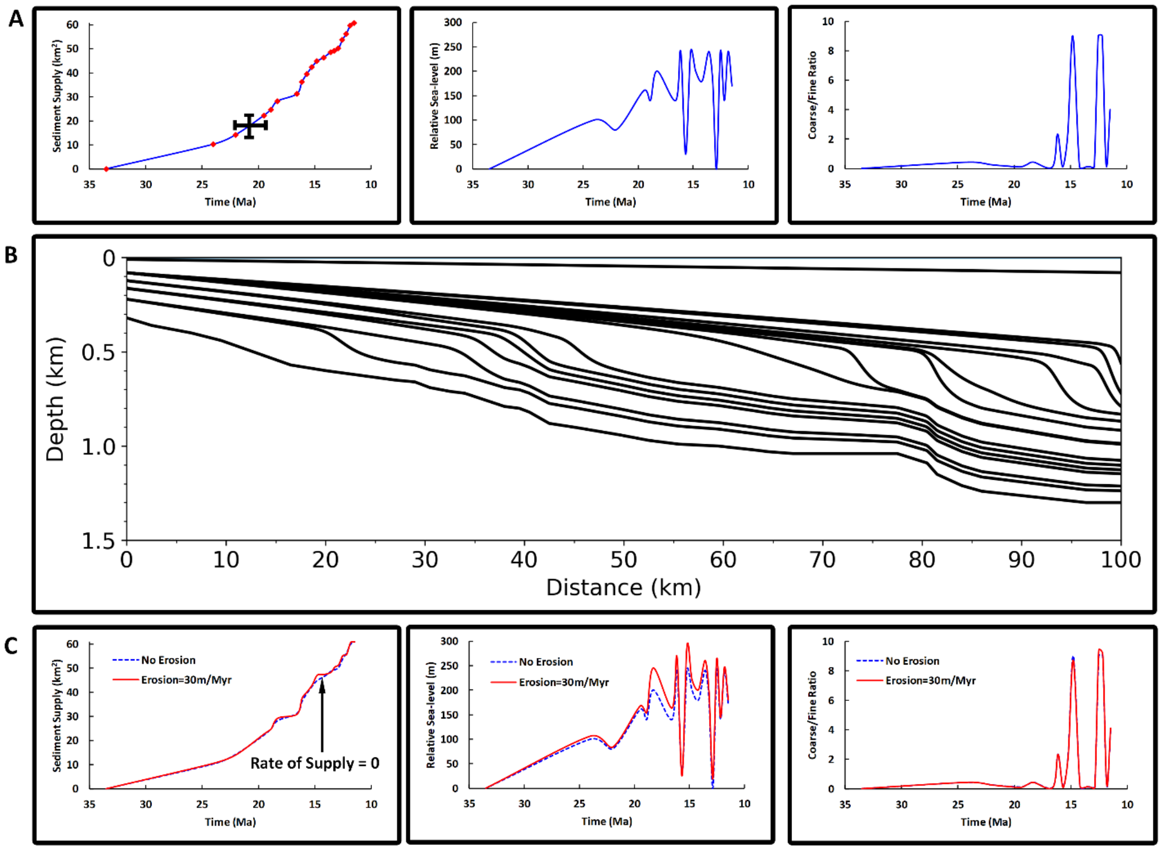

A
Sediment Supply (km²)
Time (Ma)
Relative Sea-level (m)
Coarse/Fine Ratio
B
Depth (km)
Distance (km)
C
No Erosion
Erosion=30m/Myr
Rate of Supply = 0

Figure 9